Mitigation of Mode-One Asymmetry in Laser-Direct-Drive Inertial Confinement Fusion Implosions

O. M. Mannion,[1] I. V. Igumenshchev,[1] K. S. Anderson,[1] R. Betti,[1] E. M. Campbell,[1] D. Cao,[1] C. J. Forrest,[1] M. Gatu Johnson,[2] V. Yu. Glebov,[1] V. N. Goncharov,[1] V. Gopalaswamy,[1] S. T. Ivancic,[1] D. W. Jacobs-Perkins,[1] A. Kalb,[1] J. P. Knauer,[1] J. Kwiatkowski,[1] A. Lees,[1] F. J. Marshall,[1] M. Michalko,[1] Z. L. Mohamed,[1] D. Patel,[1] H. G. Rinderknecht,[1] R. C. Shah,[1] C. Stoeckl,[1] W. Theobald,[1] K. M. Woo,[1] and S. P. Regan[1]

[1]Laboratory for Laser Energetics, University of Rochester
[2]Plasma Science and Fusion Center, Massachusetts Institute of Technology

Mode-one ($\ell = 1$) asymmetries have been identified as one of the most detrimental to inertial confinement fusion implosion performance[1] and have been observed in laser-indirect-drive implosions at the National Ignition Facility.[2] Mode-one asymmetries can be described as those asymmetries that cause the initial radial implosion velocity of the shell to have the form $v_r(\theta) = v_0 - \Delta v \cos(\theta)$, where v_0 is the average implosion velocity, Δv is the variation in the implosion velocity, and θ is the angle between the mode-one direction and a direction on the target. As the target implodes, this asymmetry causes the formation of a jet within the hot spot.[1] This jet undergoes a Helmholtz instability, which results in the formation of vortices within the hot spot and an asymmetric fuel areal density around the hot spot. The asymmetric fuel distribution leads to poor confinement of the hot spot, while the motion within the hot spot represents residual kinetic energy not used to heat and compress the target.[1] The poor confinement and residual kinetic energy present in the target result in a severe reduction in the fusion yield of the implosion.

To diagnose mode-one asymmetries in laser-direct-drive (LDD) implosions performed on the OMEGA laser, 3-D nuclear and x-ray diagnostics have been developed.[3–5] Neutron time-of-flight (nTOF) and charged-particle spectrometers are used to measure the neutron energy spectrum emitted from the target from which the fusion yield, hot-spot velocity, apparent ion temperature, and fuel areal density are inferred. X-ray imaging diagnostics are used to measure the x-ray self-emission from the hot spot and to infer the size and shape of the hot spot. These diagnostics have been fielded strategically around the OMEGA target chamber to provide a set of 3-D measurements of the hot spot and fuel conditions near peak compression. Using measurements from these diagnostics, the magnitude and direction of mode-one asymmetries are determined.

Measurements made with these detectors have revealed that large mode-one drive asymmetries can be introduced when laser-alignment errors exist. For the experiments described below, defects in the targets used for laser alignment result in the OMEGA Laser System having abnormally large laser-alignment errors. In particular, the aluminum oxide coating on the target used during the laser-alignment process had unintentional coating defects, which caused gross mispointing of the laser beams to be introduced. Furthermore, the Au spheres used during the laser-pointing procedure for these experiments had unintentional nonuniform Au coatings as a result of target fabrication issues. The nonuniform Au coating resulted in weak x-ray signals being generated by specific beams. The weak signals led to large uncertainties in identifying the position of these beams and resulted in large beam-pointing errors being introduced during the beam-pointing procedure. The compounding errors in the alignment of the laser system during these experiments resulted in a large laser mode-one asymmetry being present.

Figure 1(a) shows the laser illumination perturbation on target for shot 94712. The laser illumination on target was determined from a hard sphere calculation, which determines the overlap intensity of all 60 beams on the initial target radius, accounting for the laser beam pointing, laser beam energy, and target offset. The laser beam pointing was determined during the beam-alignment procedure prior to the shot, the laser beam energy was measured using a calorimeter, and the target offset was measured by both

(a) Shot 94712

(b) Shot 94715

Illumination perturbation (%)

Illumination perturbation (%)

E29543JR
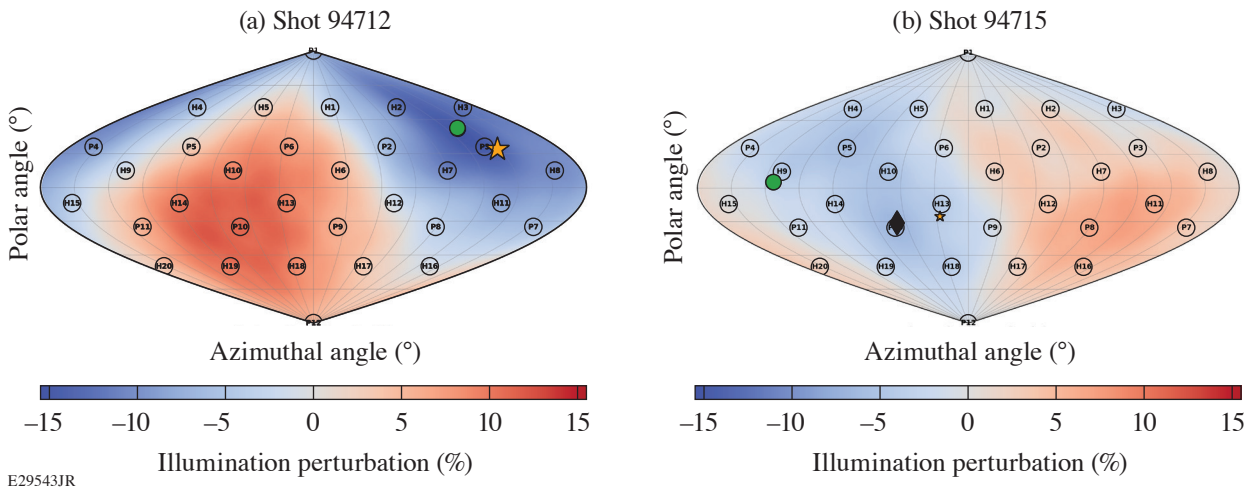
Figure 1

A sinusoidal projection of the OMEGA target chamber showing the illumination perturbation from the mean for (a) shot 94712 and (b) shot 94715 determined from a hard sphere calculation that used the measured laser beam pointing, energy, and target offset. The direction of the measured hot-spot velocity is shown as the orange star and had a magnitude of 146 km/s for shot 94712 and 27 km/s for shot 94715. The laser mode-one illumination asymmetry σ_{rms} amplitude was 7.3% for shot 94712 and 4.3% for shot 94715; the directions are shown as the green circles. The target offset correction for shot 94715 was 43 μm and is shown as the black diamond.

a high-speed video camera and an x-ray pinhole camera. For this experiment, the target offset was <5 μm and nonuniformities in the individual laser beam energies did not contribute significantly to the on-target illumination nonuniformity, which was dominated by the beam-pointing errors. The calculated on-target illumination nonuniformity shows a large mode-one drive asymmetry present with a total peak to valley variation of 27.3% across the target and a mode-one illumination asymmetry σ_{rms} amplitude of 7.3% in the direction $\theta = 51°$ and $\phi = 122°$.

This initial drive asymmetry in the laser resulted in a strong mode-one being present in the experiment, which was observed in both the nuclear and x-ray diagnostics. A hot-spot velocity of 146±12 km/s was inferred from the nTOF's in the direction $\theta = 64±7°$ and $\phi = 133±4°$. The apparent ion temperature asymmetry was 1.8±0.5 keV as measured from the nTOF detectors and the areal-density asymmetry was 104±18 mg/cm^2 as measured by the nTOF and magnetic recoil spectrometer detectors. The direction of the hot-spot velocity, apparent ion temperature asymmetry, and areal-density asymmetry were all aligned with the initial mode-one drive asymmetry identified in the laser. Furthermore, the mode-one asymmetry was observed in the x-ray self-emission images shown in Fig. 2.

(a)   (b)   (c)   (d)   (e)   (f)

25 μm   25 μm   25 μm   25 μm   25 μm   25 μm

Relative x-ray intensity (arbitrary units)
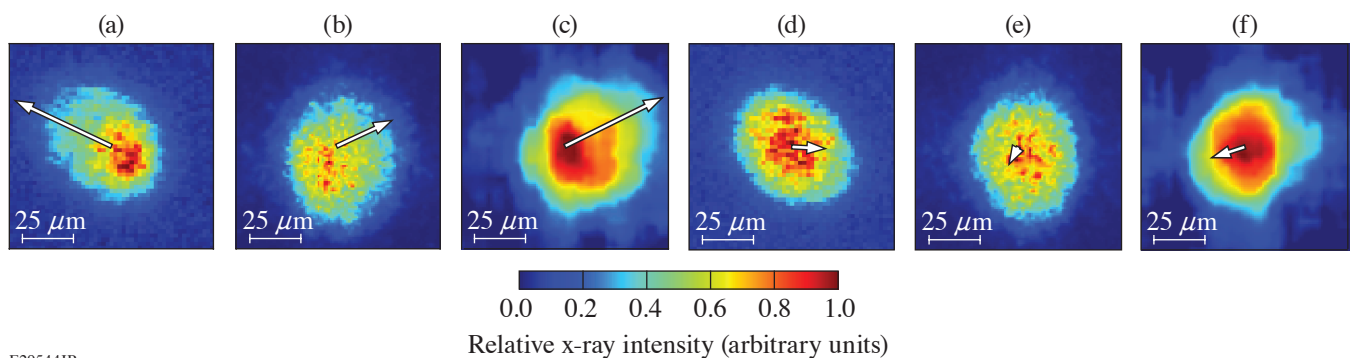
E29544JR

Figure 2

X-ray self-emission images measured for [(a)–(c)] shot 94712 and [(d)–(f)] shot 94715. The [(a) and (d)] single-line-of-sight time-resolved x-ray imager and [(b) and (e)] KBframed images are time resolved and averaged over a 40- and 15-ps time window around peak neutron production, respectively. The [(c) and (f)] gated monochromatic x-ray image is time integrated. The projection of the measured hot-spot velocity onto the detector plane is indicated by the white arrow. The magnitude of the projection is indicated by the length of the arrow. The elongation observed in the x-ray images from shot 94712 has been eliminated by applying the offset correction on shot 94715.

With the mode-one asymmetry characterized on shot 94712, we used a mitigation strategy that employed an intentional target offset to compensate for the observed asymmetry. When a target offset is present in an experiment, it results in a geometric redistribution of the beam overlap intensity on the target and can be used to mitigate mode-one drive asymmetries present in the laser. To determine the appropriate target offset required to mitigate a given mode-one observed on shot 94712, the measured hot-spot velocity was used. The hot-spot velocity $\vec{u}_{hs}$ is assumed to have a linear relationship with the target offset $\vec{o}$ and is given by

$$\vec{u}_{hs} = \alpha\vec{o} = \alpha(\vec{r} + \vec{c}), \tag{1}$$

where α is the offset-to-velocity conversion in km/s/μm, and the total offset is assumed to be the sum of the measured offset $\vec{r}$ from the high-speed video camera and some unknown effective target offset $\vec{c}$. The unknown effective target offset is the component of the hot-spot velocity generated from an assumed static mode-one present in the laser.

These calculations were performed using the results from the experiments discussed above, and the target was positioned to the calculated location to eliminate the mode-one asymmetry. The offset-to-velocity conversion for these experiments was found to be 4.1±0.2 km/s/μm. The unknown effective target offset was determined to be $\vec{c} = \langle -26, 33, 17 \rangle$ μm. This corresponds to a total target offset of 45 μm in the direction $\theta = 112°$ and $\phi = 308°$. For shot 94715, the target was positioned at $\vec{r} = \langle 28, -35, -19 \rangle$ μm, which was within a few microns away from the requested location of $\langle 26, -33, -17 \rangle$ μm. With the target positioned to this location, the asymmetry present in the previous experiments was greatly mitigated. In particular, the hot-spot velocity was reduced to 27±11 km/s in the direction $\theta = 109±35°$ and $\phi = 341±26°$ and is shown in Fig. 1(b). The apparent ion-temperature asymmetry was greatly reduced to 0.5±0.5 keV and the areal-density asymmetry was reduced to 37±12 mg/cm^2. Finally, the hot-spot x-ray self-emission images were found to be significantly more symmetric with the mode-one mitigation and are shown in Fig. 2.

To understand how this target-offset correction was able to mitigate the mode-one asymmetry, it is instructive to analyze the hard sphere illumination nonuniformity for shot 94715. Figure 1(b) shows that when the target correction was applied, the on-target illumination uniformity was improved by a factor of 2 as compared to shot 94712. In particular, the total peak-to-valley variation around the target was reduced to 14%. This technique therefore is a viable mitigation strategy for LDD implosions that have large mode-one drive asymmetries.

1. B. K. Spears *et al.*, Phys. Plasmas **21**, 042702 (2014).
2. H. G. Rinderknecht *et al.*, Phys. Rev. Lett. **124**, 145002 (2020).
3. O. M. Mannion *et al.*, Nucl. Instrum. Methods Phys. Res. A **964**, 163774 (2020).
4. F. J. Marshall *et al.*, Rev. Sci. Instrum. **88**, 093702 (2017).
5. W. Theobald *et al.*, Rev. Sci. Instrum. **89**, 10G117 (2018).